Environmental Science and Ecotechnology 26 (2025) 100593

Contents lists available at ScienceDirect

Environmental Science and Ecotechnology

journal homepage: www.journals.elsevier.com/environmental-science-and-ecotechnology/

Original Research

Microplastic pollution threatens mangrove carbon sequestration capacity

Xiaotong He [a], Shiguang Xu [a], Han Ren [a], Xiaobing Yang [a], Feizhou Su [a], Shuo Gao [a], Chenxi Xie [a], Junhui Zhao [a], Zhan Jin [a], Xiangjin Shen [b], Rongxiao Che [c], Derong Xiao [a,d,*]

[a] State & Local Joint Engineering Research Center for Ecological Treatment Technology of Urban Water Pollution, College of Life and Environmental Science, Wenzhou University, Wenzhou, Zhejiang, 325035, China
[b] Northeast Institute of Geography and Agroecology, Chinese Academy of Sciences, Changchun, 130102, China
[c] State Key Laboratory for Vegetation Structure, Function and Construction (VegLab), Institute of International Rivers and Ecosecurity, Yunnan University, Kunming, 650500, China
[d] Institute for Eco-environmental Research of Sanyang Wetland, Wenzhou University, Wenzhou, Zhejiang, 325035, China

ARTICLE INFO

Article history:
Received 23 March 2025
Received in revised form
30 June 2025
Accepted 2 July 2025

Keywords:
Microplastics
Methane microbe
Biogeochemical cycles
Carbon emission
Mangrove

ABSTRACT

Microplastics are a pervasive environmental pollutant, altering microbial communities and disrupting global biogeochemical cycles. Mangrove forests, critical blue carbon habitats, are significant sinks for microplastic accumulation, yet they also cycle large amounts of methane, a potent greenhouse gas. The effect of plastic pollution on methane dynamics in these vital habitats remains, however, poorly understood. Here we show that microplastic pollution in mangrove soils is linked to an increased potential for methane production by favouring methanogenic archaea. Through a nationwide survey of Chinese mangroves, we found that microplastic concentrations were higher (6516 ± 1725 particles kg^{-1}) in surface soils (0–20 cm) and exhibited stronger association with methane-cycling microbes (four linkage pathways), compared to concentrations (2246 ± 497 particles kg^{-1}) and two linkage pathways in deeper soils (20–40 cm). Microplastics in topsoil were correlated with more complex microbial networks, consisting of 150 nodes and 237 links, relative to 113 nodes and 196 links in deeper soils. Furthermore, we directly linked elevated microplastic pollution in surface soils to secondary industry output, which positively correlated with the methanogens-to-methanotrophs gene ratio, establishing a clear anthropogenic driver for this shift. These findings reveal a critical, previously unrecognized mechanism by which industrial plastic pollution may compromise the net carbon sequestration capacity of mangrove ecosystems. Mitigating microplastic discharge is therefore not only a waste management issue but is also essential for preserving the climate-regulating function of these crucial habitats amid global conservation efforts.

1. Introduction

Microplastics (MPs), defined as solid plastic particles measuring 5 mm or less, are emerging pollutants widely distributed across ecosystems, posing significant threats to the global biosphere [1]. Of particular concern are their substantial impacts on biogeochemical cycling, particularly carbon cycling, through their disruptive effects on microbial diversity and community structure—key drivers of these essential ecological processes [2,3]. These disruptions may lead to cascading environmental consequences [4]. The complex interactions between MPs and soil microbial communities, which fundamentally regulate biogeochemical processes, have become a critical research focus for addressing the escalating global environmental challenge [5].

MPs influence soil microorganisms through three primary mechanisms: (1) providing microbially available organic carbon [6] and forming colonizable ecocoronas, which may either stimulate [7] or inhibit [8] microbial activity; (2) inducing direct toxicity through their intrinsic properties, chemical additives, or adsorbed contaminants, thereby disrupting microbial and faunal

* Corresponding author. No. 276 Xueyuan Road, Wenzhou, Zhejiang, 325035, China.
E-mail address: xiaoderong1@163.com (D. Xiao).

https://doi.org/10.1016/j.ese.2025.100593

activity [9]; and (3) modifying soil physicochemical properties, including pH [10], aggregate stability, bulk density, and moisture retention capacity [11]. The diverse characteristics of MPs—such as polymer type, size, shape [12], and concentration [9]—have variable impacts on microbial community structures and functions [11]. Consequently, the interactions between MPs and microorganisms are highly complex and depend on the context, influenced by anthropogenic and natural factors [13,14].

Mangroves are critical blue carbon ecosystems, accounting for 10–15% of coastal carbon sequestration globally [15]. These ecosystems serve as substantial sources of methane (CH_4)—a greenhouse gas with 34 times the global warming potential of carbon dioxide (CO_2) over a century [16]—the production and consumption of which are mediated by methanogenic and methanotrophic microbial communities [17,18]. Current estimates suggest mangrove emissions of 0.34 Tg CH_4 yr^{-1}—approximately 20% of their net primary production [19]—which can potentially offset their blue carbon storage capacity [20]. Simultaneously, mangroves function as significant global sinks for MPs [21], with their dense root systems and complex aboveground structures efficiently trapping fine particulate matter [22]. The interplay between MPs and CH_4-cycling microorganisms, particularly the ratio of methanogenic (*mcrA*) to methanotrophic (*pmoA*) functional genes [17,18], serves as a critical indicator of CH_4 emission potential. This microbial balance is modulated by anthropogenic influences [23] and environmental conditions that govern MP accumulation in mangrove soils [24]. Despite the ecological significance of these interactions, research addressing the complex relationships between MPs and CH_4-cycling microbial communities in mangrove ecosystems remains notably limited [13].

Global mangrove coverage has declined by over one-third in the past six decades [25], posing substantial challenges to climate change mitigation efforts [26]. To preserve their critical carbon sequestration capacity, international mangrove restoration initiatives aim to achieve a 20% increase in global coverage by 2030 [27]. Notable Indonesian efforts include a national target to restore 600,000 ha of mangroves by 2024 [28], and China has a national plan to rehabilitate 18,800 ha by 2025 [29]. However, these restoration activities may inadvertently alter MP accumulation patterns and their interactions with CH_4-cycling microbial communities, potentially influencing CH_4 emissions. Understanding these complex relationships is crucial for optimizing ecosystem management during restoration projects and for offering opportunities to mitigate CH_4 emissions while enhancing carbon sequestration potential.

In this study, we examined the complex interactions between MPs and CH_4-cycling microorganisms across China's mangrove ecosystems (19.84°–28.35° N) (Supplementary Fig. S1), encompassing diverse climatic conditions and anthropogenic pressures. Focusing on soil systems as primary MP reservoirs [22], we addressed three key aspects: (1) spatial distribution and composition of MPs in topsoil (0–20 cm) and subsoil (20–40 cm) layers, (2) structure and abundance of methanogenic and methanotrophic microorganism communities, including functional (*mcrA* and *pmoA*) genes, and (3) interactions between MPs and microbial communities under varying anthropogenic (industrial output across economic sectors) and environmental (climatic and edaphic) conditions. By integrating these components, we aimed to clarify how MP pollution influences CH_4-cycling microbial communities in mangroves, considering the synergistic effects of climate, soil properties, and human activities while addressing the growing threat of MP contamination in global mangrove areas.

2. Materials and methods

2.1. Study areas and sample collection

Mangroves predominantly colonize the intertidal zones of China's southeast coast, spanning 18.2–29.5° N and covering approximately 14,700 km of coastline [30]. This region is characterized by a tropical and subtropical monsoon climate with hot, rainy summers and warm, humid winters. The mean annual temperature (MAT) ranges from 21 to 25 °C, with the coldest monthly average varying between 7.4 and 21.0 °C. Annual precipitation averages 1200–2200 mm, resulting in high humidity. The coastline features a mix of muddy, sandy, and rocky shores with diverse tidal patterns. The total mangrove area is approximately 28,010 ha [30], varying from concentrated patches of mangroves at lower latitudes to scattered distributions at higher latitudes [31].

Sample collection was conducted in July 2023 at 14 representative mangrove sites along a latitudinal gradient covering the coastline bordering the Hainan (HN), Guangdong (GD), Guangxi (GX), Fujian (FJ), and Zhejiang (ZJ) provinces (Supplementary Fig. S1). At each site, we established a 20 m × 20 m transect, within which we placed three 2 m × 2 m quadrats diagonally at intervals of 8 m. Before sampling, we measured environmental variables, including soil conductivity, electrical conductivity, and temperature, at each site using a ProCheck multi-parameter meter (METER Group, Inc., Pullman, WA, USA), and recorded the geographic coordinates using global positioning system (GPS).

To minimize plastic contamination during soil sampling, we used stainless steel cutting rings (7 cm in diameter and 5 cm in height), employing separate rings to collect stratified samples from the topsoil (0–20 cm) and subsoil (20–40 cm) layers. We mixed the samples collected from each quadrat according to their respective depths and immediately placed them into aluminum foil containers cleaned with ultrapure water. From these collections, we obtained three sets of samples for specific analyses: one for MP determination, another for assessing soil physicochemical properties, and a third for analyzing CH_4-cycling microorganisms.

2.2. MP analysis

In this study, we categorized MPs into two primary groups based on their physical properties (e.g., shape, color, and size) and chemical composition, with a focus on polymer types. We classified shapes into fibers, fragments, foams, and pellets, and divided colors into black, white, blue, green, and other categories. Size classifications included microscopic MPs (<1 mm) and visible MPs (1–5 mm). The identified polymer types were polyethylene (PE), polyester (PET), polystyrene (PS), and polypropylene (PP). Notably, we labeled fibers anthropogenic when dyes prevented polymer identification.

Similarly, to minimize plastic contamination, personnel wearing cotton lab coats performed all handling of samples on aluminum foil-covered surfaces using only glassware meticulously cleaned with three rinses of ultrapure water. MPs were primarily identified through a combination of density separation using zinc chloride, oxidation digestion, and visual inspection. The process began by wet-sieving the samples on a 200-mesh screen to ensure size limits, followed by flotation in a 100 mL solution of $ZnCl_2$. Samples were then digested with 30% H_2O_2 at 60 °C for 12 h to remove organic matter and biological contaminants. After digestion, samples were filtered through a Whatman® 0.45-μm glass

microfiber filter (Gf/f-grade, 47 mm in diameter, Cytiva, Marlborough, MA, USA) and stored in a clean glass Petri dish. MPs were visually inspected under a dissecting microscope (40 ×, Wild M3Z, Wild Heerbrugg AG, Heerbrugg, Switzerland) to identify shapes and colors, including red, orange, and yellow. For ambiguous classifications, we employed fourier transform infrared spectroscopy (FTIR) analysis using a Thermo Fisher Scientific™ Nicolet™ iN10 instrument (Thermo Fisher Scientific, Wisconsin, USA), comparing the obtained spectra against a standard polymer library using OMNIC software, classifying samples with over 70% match as microplastics.

2.3. Deoxyribonucleic acid extraction and sequencing

Microbial deoxyribonucleic acid (DNA) was extracted from approximately 0.25 g (wet weight) of each soil samples using an E.Z.N.A.® Soil DNA Kit (Omega Bio-tek Inc., Norcross, GA, USA). DNA quality was evaluated using a NanoDrop™ 2000 spectrophotometer (Thermo Fisher Scientific, USA), and quantity was confirmed using 1.0% agarose gel electrophoresis.

For the methanogenic archaea community, the *mcrA* genes were amplified using primers *mcrA*-f (5′-GGTGGTGTMGGATTCACACARTAYGCWACAGC-3′) and *mcrA*-R (5′-TTCATTGCRTAGTTWGGRTAGTT-3′). The methanotrophic bacterial communities were examined by amplifying *pmoA* genes using primers A189F (5′-GGNGACTGGGACTTCTGG-3′) and MB661R (5′-CCGGMGCAACGTCYTTACC-3′). To facilitate sample identification, the primers were tagged with PacBio barcode sequences. The amplification reactions (20-μL volume) included 10 μL of 2 × Taq Plus Master Mix, 0.8 μL of forward primer (5 μM), 0.8 μL of reverse primer (5 μM), and 7.4 μL of DNase-free water. Polymerase chain reaction (PCR) was conducted following initial denaturation at 95 °C for 5 min, followed by 30 cycles of 95 °C for 30 s, 58 °C for 30 s, and 72 °C for 1 min (extension) on a T100™ thermal cycler (BIO-RAD, CA, USA). After electrophoresis, PCR products were purified using AMPure® PB beads (Pacific Biosciences, CA, USA) and quantified with Qubit 4.0 Fluorometer (Thermo Fisher Scientific, MA, USA) (Supplementary Table S1).

Purified amplicons were pooled in equimolar amounts and paired-end sequenced using an Illumina NextSeq 2000 sequencing system (Illumina, CA, USA), following the established protocols of Majorbio Bio-Pharm Technology Co., Ltd. (Shanghai, China). Following sequencing, the raw FASTQ files were demultiplexed using an in-house Perl script and quality-filtered with fastp version 0.19.6. Merging was performed with Flash version 1.2.7 according to the following criteria: (1) reads truncated at any position where the average quality score fell below 20 over a 50 bp sliding window; no truncated reads shorter than 50 bp or any containing ambiguous characters; (2) assembly of only overlapping sequences exceeding 10 bp in length based on their overlap, with a maximum matching ratio of 0.2 for the overlapped region; no reads that failed to assemble; (3) samples distinguished by barcode and prime sequences, with adjustments made for sequence direction, allowing for exact barcode matches and up to two nucleotide mismatches in primer matching.

The optimized sequences were clustered into operational taxonomic units (OTUs) using UPARSE 7.1 with a 97% sequence similarity threshold. The most abundant sequence for each OTU was designated as the representative sequence. To mitigate the effects of sequencing depth on alpha and beta diversity metrics, the counts of *mcrA* and *pmoA* gene sequences for each sample were rarefied to 20,000, ensuring an averagely good coverage of 99.09%. The taxonomy of each OTU representative sequence was analyzed using RDP Classifier version 2.2 against the 16S rRNA gene database (Silva v. 138), with a confidence threshold of 0.7.

2.4. Dataset of human impacts and environmental variables

The 14 sampling sites were grouped by county, encompassing Wenchang City in HN, Leizhou City District in GD, and Mazhang District in GD, among others (Supplementary Table S2). Industry output values for the primary (agriculture-dominated), secondary (industry-dominated), and tertiary (services-dominated) sectors were obtained from annual yearbooks (2018–2022) [32–36]. Five-year averages were calculated and employed as quantitative parameters to assess the type and intensity of human disturbances at the sites. We designated temperature and precipitation as key indicators of climatic influence. Specifically, MAT and mean annual precipitation (MAP) were sourced from the World Climate website (www.worldclimate.com) using the geographic coordinates (latitude and longitude) of the sampling locations. The dataset provided a spatial resolution of 1 km and an absolute resolution of 0.86 [37], providing precise characterization of the climatic conditions at the sampling sites.

We characterized the physicochemical properties of the soil samples to identify the key soil factors that influenced MP dynamics. Specifically, pH was measured using a pH meter (SevenCompact210, Mettler-Toledo, Columbus, OH, USA) with a soil-to-water ratio of 1:2:5 (w/v). The moisture content (%) was determined by oven drying at 105 °C for 24 h using a volumetric ring. Particle size distribution (%) was analyzed with a Mastersizer 2000 laser particle size analyzer (Malvern Scientific Instruments, Malvern, UK). Soil organic carbon (SOC) (g kg^{-1}) was quantified through H_2SO_4–$K_2Cr_2O_7$ oxidation, followed by titration with $FeSO_4$. Total nitrogen (TN, g kg^{-1}) and total phosphorus (TP, g kg^{-1}) were analyzed according to the methods described by Bao [38]. Each sample was analyzed in triplicate, and average values were calculated.

Overall, our classification framework facilitated the categorization of the driving factors of human impact, climate, and soil parameters, thereby facilitating a comprehensive analysis of the mechanisms governing MP distribution within Chinese mangrove soils.

2.5. Data analysis

We employed Wilcoxon rank-sum tests to compare differences in the abundance of MPs, *mcrA*, and *pmoA* genes, and the *mcrA*/*pmoA* ratio between the topsoil and subsoil layers due to non-normal distributions and heteroscedasticity that violated the assumptions of paired Student's *t*-tests. Nonmetric multidimensional scaling (NMDS) was utilized to compare the compositions of MPs and microbial communities at both depths. Significance was assessed using permutational multivariate analysis of variance (Adonis) and analysis of similarity (ANOSIM), with $p < 0.05$ indicating statistical significance. All statistical analyses were performed using R software (v. 4.3.3).

Co-occurrence network analyses based on Spearman's rank correlations were employed to examine the relationships between methanogens and methanotrophs. Co-occurrence patterns were identified through strong correlations (Spearman's $\rho > |0.8|$) that were statistically significant ($p < 0.01$) [39], with *p*-values adjusted for multiple comparisons using the false discovery rate (FDR) [40]. Network visualizations were generated with Gephi (https://gephi.org/) using the Fruchterman–Reingold layout. Topological properties (e.g., degree and modularity) were calculated for both observed networks using the igraph package (v. 2.0.3) in R (v. 4.3.3). High-degree nodes were identified as key species, categorized based on their topological roles into module hubs (Zi > 2.5), network hubs (Zi > 2.5 and Pi > 0.62), connectors (Zi < 2.5 and Pi > 0.62), and peripherals (Zi < 2.5 and Pi < 0.62) [41]. This

analysis highlighted differences in interaction patterns between methanogenic archaea and methanotrophic bacterial communities at different depths. The influence of MP factors on CH_4-cycling microbial community assemblies across soil layers was further evaluated using the Mantel test with 999 permutations.

Additionally, we employed structural equation modeling (SEM) to investigate the effects of human impacts, climate, and soil conditions on the interactions between MPs and CH_4-cycling microorganisms. Some environmental variables were excluded due to high correlations with other variables (Pearson's $r > 0.8$). For the SEM of MPs and CH_4-cycling microorganisms in the topsoil, we included anthropogenic fiber, PET, soil temperature, nitrogen: phosphorus (N:P) ratio, clay content, and industrial values from the primary and secondary sectors. For the subsoil analysis, we selected variables that included black MPs, soil organic carbon (SOC) content, clay content, and primary sector outputs. The SEM was conducted using the lavaan (v. 0.6–18) package in R, and the model fit was evaluated using the chi-squared test (χ^2), *p*-value, and root mean square error of approximation (*RMSEA*).

3. Results

3.1. Abundance and composition of MPs

The abundance of MPs varied significantly, with concentrations ranging from 811 to 21,921 particles kg^{-1} in the topsoil and from 186 to 7456 particles kg^{-1} in the subsoil. The average concentration of MPs in the topsoil was 6516 ± 1725 particles kg^{-1}, significantly exceeding the subsoil average of 2246 ± 497 particles kg^{-1} (Fig. 1a).

Overall, soil depth significantly influenced the shapes, sizes, and polymer compositions of the MPs (Fig. 1b and c; Supplementary Fig. S2). Specifically, color composition varied with depth, encompassing white, blue, black, green, transparent, and other hues, with white being the most prevalent at both depths (Fig. 1b) and significant variations observed at different depths (Fig. 1c). The size distribution predominantly comprised MPs of less than 1 mm across the two groups (Fig. 1b), with their concentrations also significantly affected by depth (Fig. 1c). In contrast, the shape and polymer compositions at both depths were primarily dominated by fragments and PE (Fig. 1b), with depth having no significant influence on these traits (Fig. 1c; Supplementary Fig. S2).

3.2. CH_4-cycling microbes and their functional genes

In total, we obtained 1,076,099 and 1,186,228 high-quality *mcrA* and *pmoA* sequences, respectively. The *mcrA* sequences were classified into 5035 OTUs across 31 genera, while the *pmoA* sequences were categorized into 3944 OTUs across 25 genera (Supplementary Table S3). Notably, the alpha (α) diversity of CH_4-cycling microbial communities showed no significant differences between the topsoil and subsoil samples (Supplementary Fig. S3).

The abundance of the *mcrA* gene in the topsoil was 2.6×10^6 copies g^{-1}, with an *mcrA*:*pmoA* ratio of 2:1, both lower than in the subsoil, which had 2.7×10^6 copies g^{-1} and a ratio of 3:1. Conversely, the abundance of the *pmoA* gene in the topsoil was 2.7×10^6 copies g^{-1}, exceeding the 2.6×10^6 copies g^{-1} found in the subsoil; however, these differences were not statistically significant (Fig. 2a).

Methanolobus, *Methanosarcina*, and *Methanobacterium* were the dominant genera in the methanogenic communities at both depths, with greater abundance in the topsoil than in the subsoil. Conversely, *Methylocystis* and *Methylocaldum*, the dominant genera in the methanotrophic communities, were less abundant in the topsoil than in the subsoil (Fig. 2b). Soil depth significantly influenced the structure of the methanogenic communities but did not significantly affect the methanotrophic communities or the overall CH_4-cycling microbiota, as revealed by NMDS based on Bray–Curtis dissimilarity analysis (Fig. 2c; Supplementary Fig. S4).

The co-occurrence networks of CH_4-cycling microorganisms showed that the topsoil networks had higher numbers of nodes and links and greater modularity (Fig. 3a) than those in the subsoil (Fig. 3b). Furthermore, the topsoil exhibited a higher clustering coefficient and shorter path length, with connectors present at both depths—more prevalent in the topsoil—while a module hub was uniquely identified in the subsoil (Supplementary Table S4).

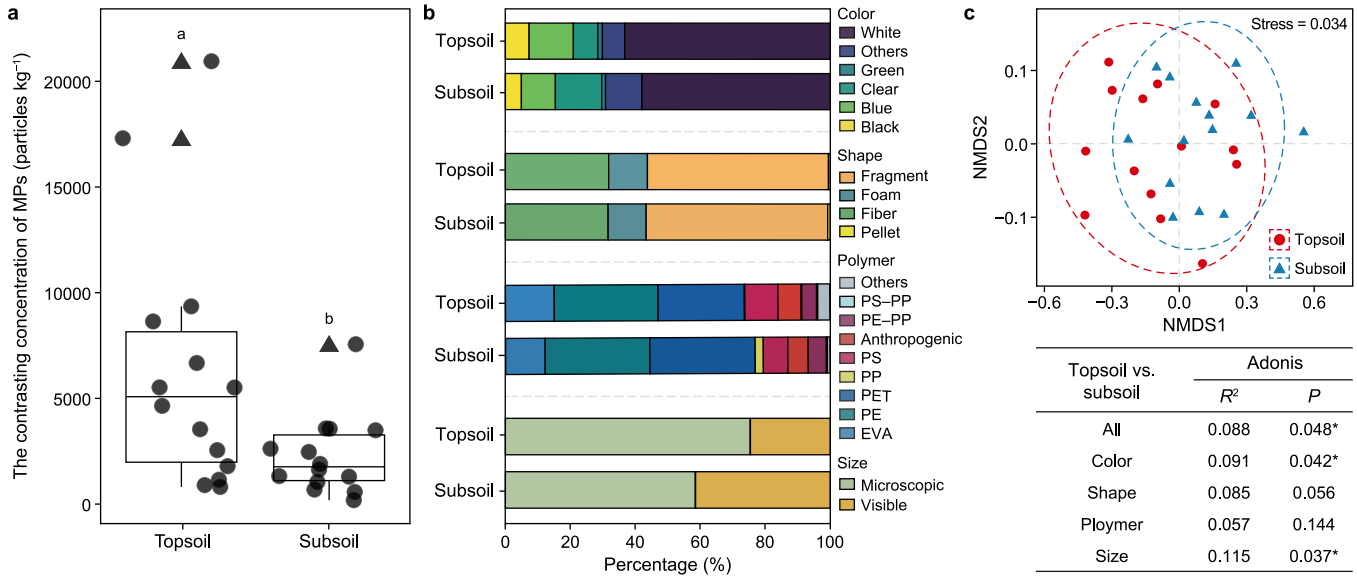

Topsoil vs. subsoil	Adonis	
	R^2	*P*
All	0.088	0.048*
Color	0.091	0.042*
Shape	0.085	0.056
Ploymer	0.057	0.144
Size	0.115	0.037*

Fig. 1. Characteristics of microplastics (MPs) in soils across China's mangroves. **a**, Box plots showing the contrasting concentration of MPs (particles kg^{-1}) between topsoil and subsoil. Data points beyond the whisker endpoints are identified as outliers and indicated by triangles. Circle: the concentration of MPs (particles kg^{-1}). **b**, Physical characteristics (color, shape, polymer, and size) and chemical composition of MPs (particles kg^{-1}) in topsoil and subsoil. **c**, Comparative analysis of the physical and chemical compositions of MPs at topsoil (0–20 cm) versus subsoil (20–40 cm). *$p < 0.05$. The MP polymers include: ethylene-vinyl acetate (EVA), polyethylene (PE), polyester (PET), polypropylene (PP), polystyrene (PS), anthropogenic fiber (Anthropogenic), polyethylene–polypropylene (PE–PP), polystyrene–polypropylene (PS–PP).

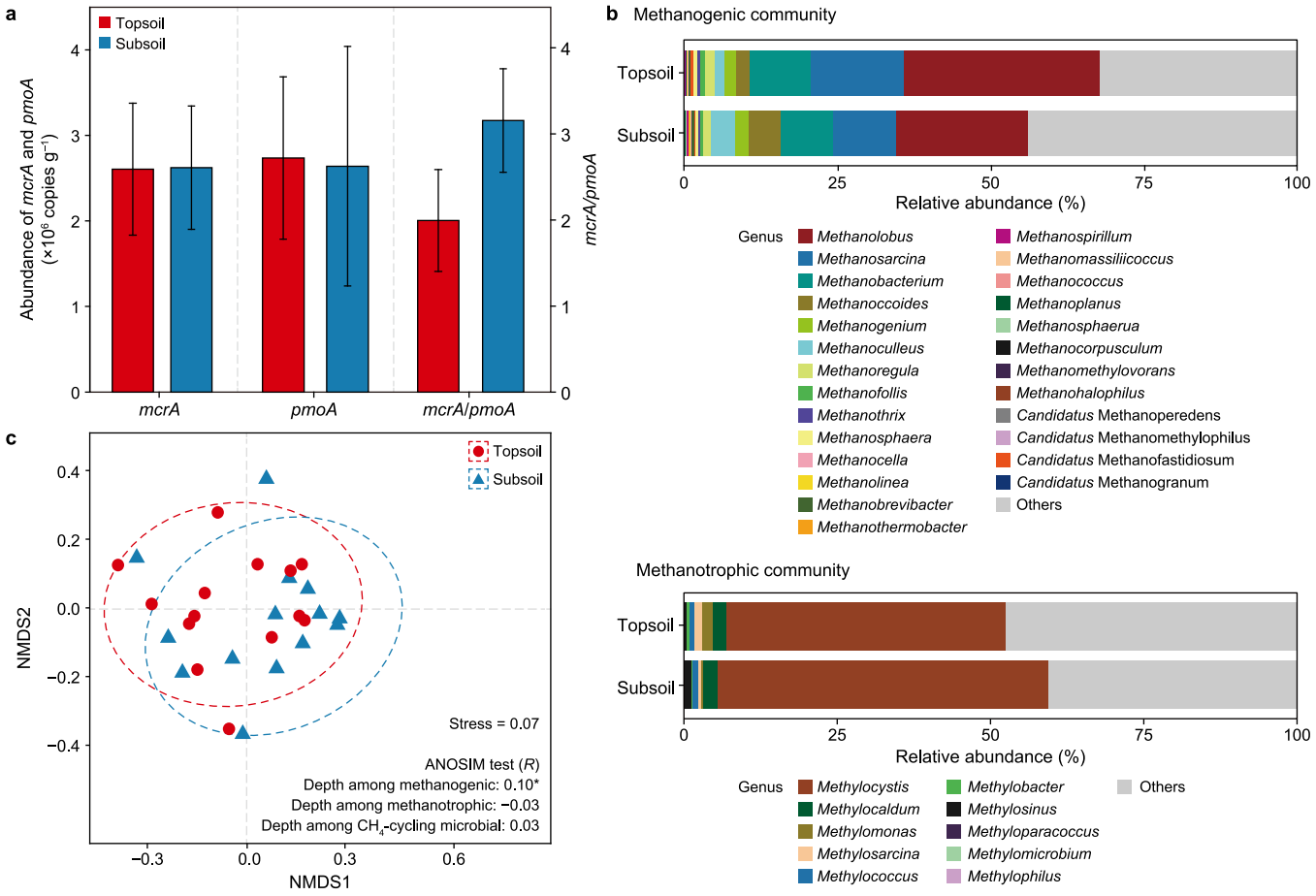

Fig. 2. Community composition and diversity of CH_4-cycling microorganisms in soils at varying depths across China's mangroves. **a**, Abundance of *mcrA* and *pmoA*, as well as the ratio of *mcrA*/*pmoA* in both topsoil (0–20 cm) and subsoil (20–40 cm) layers. **b**, Composition of methanogenic and methanotrophic communities at the genus level. **c**, Non-metric multidimensional scaling (NMDS) analysis based on Bray–Curtis distance.

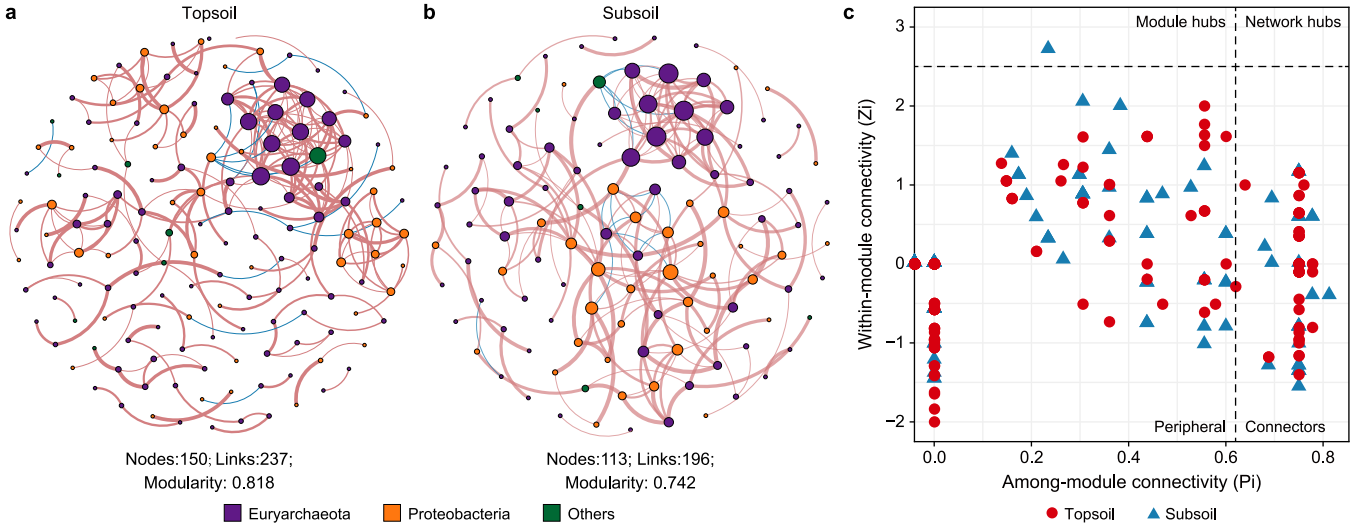

Fig. 3. a–b, Co-occurrence networks of CH_4-cycling microorganisms in topsoil (**a**) and subsoil (**b**) across China's mangroves, derived from Spearman analysis of operational taxonomic unit (OTU) profiles. The threshold values for categorizing OTUs based on Zi and Pi were set at 2.5 and 0.62, respectively. Each node in the network represents an OTU, with node size reflecting its degree of connectivity. Pink-colored lines indicate positive interactions, while blue lines denote negative interactions. The network is color-coded at the phylum level, with Euryarchaeota representing methanogens and Proteobacteria representing methanotrophs. **c**, Zi–Pi plots of methanogenic and methanotrophic communities, emphasizing their topological roles within the networks.

3.3. Interactions between MPs and CH_4-cycling microbes

The relationship between MPs and CH_4-cycling community structure was more pronounced in the topsoil than in the subsoil (Fig. 4). Specifically, the methanogenic communities in the topsoil displayed significant positive correlations with various MP characteristics, including color (white), shape (fragments), chemical composition (EVA), and size (microscopic MPs). In contrast, the methanotrophic communities showed no significant correlations with any of the MP characteristics. In the subsoil, both methanogenic and methanotrophic communities exhibited significant positive correlations exclusively with the chemical compositions of MPs, particularly PP, and polystyrene–polypropylene (PS–PP). Notably, four strong pathways linked methanogenic activity to MPs in the topsoil, while only one weak association was observed in the subsoil (Fig. 4).

MPs were associated with the functional characteristics of CH_4-cycling microbial communities, exhibiting stronger and more complex correlations with methanogenic archaea than with methanotrophic bacteria, with both relationships depending on depth (Fig. 5). For methanogenic archaea, MP properties, such as black, green, white, fragmented, and PE, exhibited significant correlations with the methanogenesis-using formate in the topsoil, whereas no significant relationships were observed in the subsoil (Fig. 5a). In contrast, only the EVA of MPs showed significant correlations with methylotrophy, methanotrophy, and the hydrocarbon degradation of methanotrophic bacteria in the subsoil (Fig. 5b).

3.4. Anthropogenic and environmental drivers of the mcrA:pmoA ratio

SEM revealed that human impacts, particularly in the primary and secondary sectors, significantly influenced the presence of MPs in the topsoil. Specifically, the primary sector had a negative effect (path coefficient = −0.57), while the secondary sector had a positive impact (path coefficient = 0.88) (Fig. 6a). In contrast, the primary sector remained the main driver of MPs in the subsoil, albeit with a lower level of significance (path coefficient = 0.32) (Fig. 6b). Climate factors, particularly MAT, positively impacted the chemical composition of MPs (PET) in the topsoil (Fig. 6a) while enhancing the physical composition of MPs (black) in the subsoil (Fig. 6b). Soil characteristics, especially clay content, negatively affected the MPs in both layers (Fig. 6a and b).

The impact of MPs on the *mcrA*:*pmoA* ratio exhibited distinct patterns across soil layers. In the topsoil, the chemical composition of anthropogenic MPs was positively correlated with the *mcrA*:*pmoA* ratio (Fig. 6a). Conversely, in the subsoil, the ratio was adversely affected by the physical characteristics of the microscopic MPs (Fig. 6b). Climate factors, particularly MAP, significantly negatively influenced the *mcrA*:*pmoA* ratio in the topsoil (path coefficient = −0.82) (Fig. 6a) but had no significant effect in the subsoil (Fig. 6b). Additionally, soil conditions directly affected the *mcrA*:*pmoA* ratio: In the topsoil, both temperature and the N:P ratio exerted negative effects (Fig. 6a), while clay content adversely affected the ratio in the subsoil (Fig. 6b). Overall, among the factors influencing the *mcrA*:*pmoA* ratio, anthropogenic MPs exhibited the most significant positive impact in the topsoil, with Soil temperature (ST)emerging as the primary negative factor (Fig. 6c). In the subsoil, MAT had the most notable positive influence, while microscopic MPs had the greatest negative effect (Fig. 6d).

4. Discussion

4.1. Divergent abundance and composition of MPs across soil depths

We observed an average MP abundance of 4381 particles kg^{-1} in mangrove soils (0–40 cm) across China, which markedly exceeded

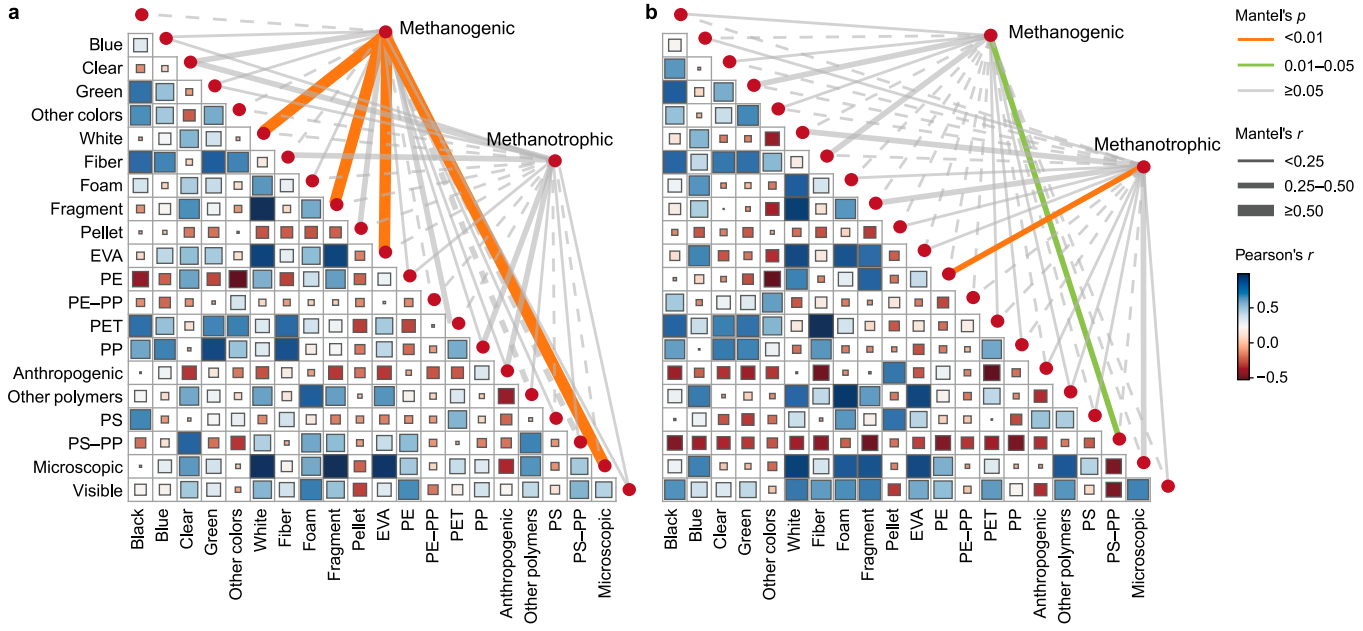

Fig. 4. Relationship between microplastics (MPs) and CH_4-cycling microorganisms in China's mangrove soils. The correlations are based on Bray–Curtis distances of the CH_4-cycling microbial community with MPs in the topsoil (**a**) and subsoil (**b**). The width of the lines corresponds to Mantel's *r* value, while the color indicates statistical significance. Solid lines denote positive correlations, while dashed lines represent negative correlations. Pairwise correlations among these variables are illustrated, with color gradients reflecting Pearson's correlation coefficients. EVA: ethylene-vinyl acetate; PE: polyethylene; PE–PP: polyethylene–polypropylene; PET: polyester; PP: polypropylene; Anthropogenic: anthropogenic fiber; PS: polystyrene; PS–PP: polystyrene–polypropylene.

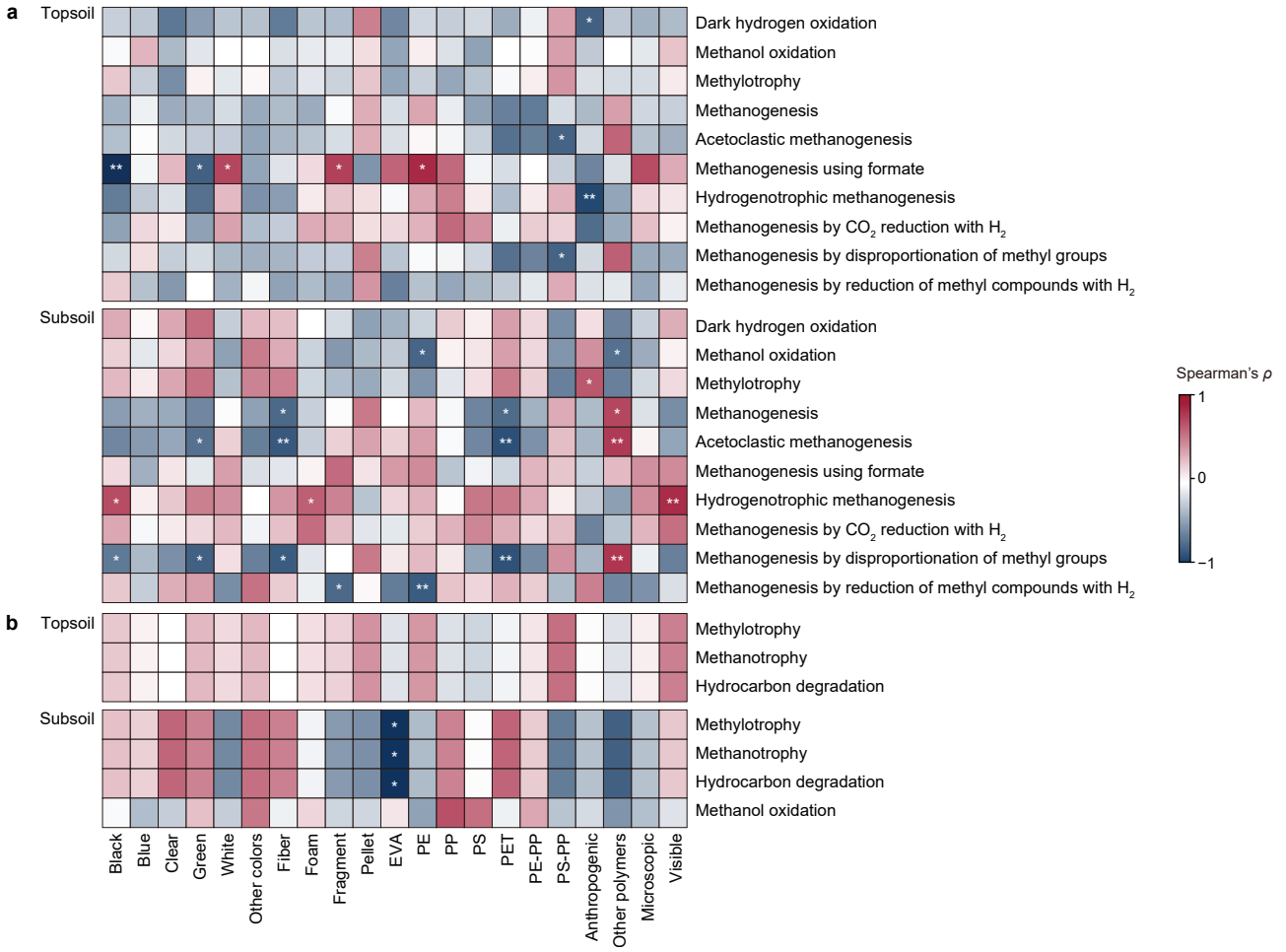

Fig. 5. Correlation heatmap between microplastics (MPs) and methanogenic (**a**) and methanotrophic (**b**) eigengenes in two layers of mangrove soil. Correlations among these variables are illustrated, with color gradients reflecting Spearman's correlation coefficients. *$p < 0.05$, **$p < 0.01$. EVA: ethylene-vinyl acetate; PE: polyethylene; PE–PP: polyethylene–polypropylene; PET: polyester; PP: polypropylene; Anthropogenic: anthropogenic fiber; PS: polystyrene; PS–PP: polystyrene–polypropylene.

the levels reported at non-mangrove sites (saltmarshes, seagrasses, and tidal flats) across the same distribution range (Table 1). This highlights mangroves' enhanced capacity to trap MPs, driven by their function as critical ecological buffers at the land–sea interface, where high primary productivity and complex hydrodynamic regimes facilitate fine particle accumulation [21].

Our study revealed a significant decrease in MP abundance with increasing depth in mangrove soils (Fig. 1b), accompanied by substantial alternations in color and size (Fig. 1c). The elevated MP concentration in topsoil is largely driven by the physical attenuation of hydrodynamic forces imposed by dense aboveground vegetation and intricate root networks, which reduce water flow velocity and promote the deposition of fine particles sourced from terrestrial and marine environments [42]. Conversely, the decline of MPs in deeper layers reflects filtration losses during vertical transport from topsoil, driven by a complex interplay of physical, chemical, and biological processes. Specifically, biodegradation due to microbial activity [43], absorption and transformation by root systems [44], removal through tidal flushing [45], and ingestion by marine organisms [46,47] facilitate the redistribution of MPs. These processes not only alter the physical characteristics of MPs—such as their size, shape, and color—but also affect their chemical bonds [43]. Consequently, MP abundance decreases with depth, accompanied by significant transformations in MPs' physicochemical properties. The observed higher MP abundance in surface soils compared to subsurface soils aligns with previous findings from both non-mangrove habitats [48,49] and localized mangrove sites [22,50].

4.2. CH_4-cycling microbes and their associations with MPs across soil depths

We observed that the relative abundance of *mcrA* genes increased with soil depth, while *pmoA* gene abundance exhibited an inverse trend, consistent with previous localized studies [51]. This pattern can primarily be attributed to the reduced oxygen (O_2) availability in the subsoil [52,53]. Moreover, the composition of the methanogenic communities was clearly dependent on soil depth, whereas the composition of the methanotrophic communities remained relatively stable. This suggests that methanogenic communities are more sensitive to MP changes with increasing soil depth. Given that CH_4 emissions largely depend on the balance between methanogens and methanotrophs [16,54], the observed 58.3% increase in the *mcrA*:*pmoA* ratio in subsoil compared to topsoil suggests a heightened potential for CH_4 production.

Our results recorded variations in dominant genera across soil depths (Fig. 2b), indicating that different species within these communities respond uniquely to environmental changes according to soil layer conditions, such as increased pH and salinity, which affect both methanogenic and methanotrophic populations [55,56]. Moreover, the finding that soil depth significantly

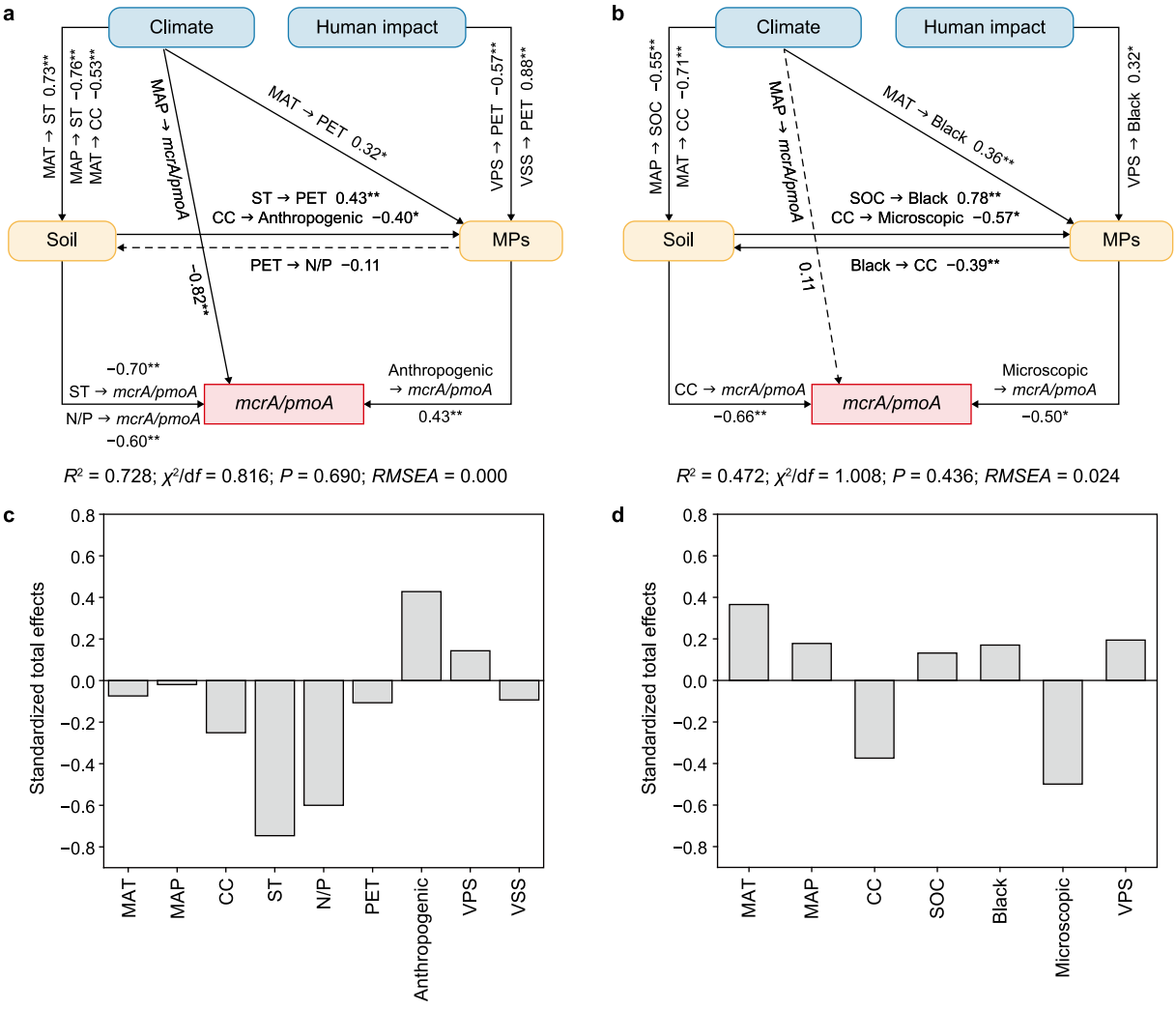

Fig. 6. Structural equation models (SEMs) illustrating the hypothesized direct and indirect relationships between human activities, climate, soil conditions, microplastics (MPs), and the *mcrA/pmoA* ratio. **a**–**b**, The relationships in the topsoil (**a**) and subsoil (**b**). Predictors are represented as independent observable variables grouped within a single box for clarity rather than as latent variables. Solid arrows represent statistically significant associations (two-sided $^{**}p < 0.05$), with adjacent correlation coefficients; dashed arrows indicate non-significant associations. **c**–**d**, The standardized total effects from SEMs in the topsoil (**c**) and subsoil (**d**). MAT: mean annual temperature (°C); MAP: mean annual precipitation (mm); CC: clay content (%); ST: soil temperature (°C); SOC: soil organic carbon (g kg^{-1}); PET: polyester; VPS: values of the primary sector (in RMB 100 million); VSS: value of the secondary sector (in RMB 100 million). $^{*}p < 0.05$; $^{**}p < 0.01$.

Table 1
Summary of microplastic abundance in mangrove and adjacent non-mangrove habitats (tidal flats, saltmarshes, seagrasses) across mangrove distribution provinces in China.

Sites	Location	Microplastic abundance (particle kg^{-1})	Reference
Tidal flat	Guangxi	3266	[80]
Tidal flat	Guangdong, Guangxi, Hainan	3200	[81]
Tidal flat	Fujian	311	[82]
Tidal flat	Zhejiang	408	[83]
Tidal flat	Guangdong	344	[84]
Seagrass	Hainan	780	[85]
Seagrass	Hainan	197	[85]
Seagrass	Guangxi	214	[86]
Seagrass	Guangxi	45	[86]
Saltmarsh	Zhejiang	693	[83]
Saltmarsh	Zhejiang	180	[87]
Saltmarsh	Zhejiang	230	[87]
Saltmarsh	Zhejiang	150	[87]
Mangrove	14 counties across China (Hainan, Guangxi, Guangdong, Fujiang, Zhejiang)	4381	This study

influenced the structure of methanogenic communities while exerting no significant impact on methanotrophic communities or the overall CH_4-cycling microbiota (Fig. 2c; Supplementary Fig. S3) indicates that methanogenic communities are more sensitive to environmental changes associated with soil depth than their methanotrophic counterparts. The heightened sensitivity of methanogens stems from their specific metabolic pathways tied to substrate availability and environmental conditions, while the reduced sensitivity of methanotrophic bacteria results from their broader tolerance to varying environments [57,58].

The more complex microbial network indicated less intense competition among microorganisms in the topsoil than in the subsoil (Fig. 3a and b), which was largely influenced by environmental conditions and the structures of bacterial communities [59,60]. Additionally, the higher proportion of positive interactions in the topsoil suggests more efficient substrate transport and information transfer between genera in the methanogen –methanotroph interaction network, facilitated by cooperative symbiosis between genera [61].

MPs impact soil microbial communities in mangrove habitats. However, existing knowledge primarily derives from laboratory studies employing artificial MP additions, which yield inconsistent impacts—positive [62–64], negative [65–67], or neutral [68,69]—on microbial assemblages. This variability highlights the complex, context-dependent, and poorly understood nature of MP–microbe interactions in such soils.

In this study, we revealed correlations between MPs and methanogenic activity, with four strong pathways identified in the topsoil and only one weak association in the subsoil (Fig. 4). These depth-dependent relationships can largely be attributed to variations in physical traits—such as size, shape, and color—as well as MPs' chemical compositions [70,71], suggesting that the influence of MPs on methanogenic processes diminishes with soil depth. In addition, we observed stronger and more complex correlations between MPs and methanogenic archaea compared to methanotrophic bacteria, both of which were depth-dependent (Fig. 5). This suggests that methanogenic communities are more sensitive to MPs than methanotrophic communities at both depths, probably due to the substrate-limited metabolic pathways of methanogenic microbes [58]. Collectively, these findings provide further evidence that, under natural conditions, MPs in mangrove soils exhibit depth-dependent interactions with CH_4-cycling microbial communities, exerting a more pronounced and complex effect on CH_4 production than on CH_4 oxidation.

4.3. Factors and pathways influencing the associations between MPs and CH_4-cycling microbes

The results revealed that the agriculture-dominated primary sector negatively impacts MPs (Fig. 6), suggesting a mitigating effect on the influx of MPs into mangroves due to their interception and continuous breakdown of MPs through mechanical crushing, photodegradation, physical weathering, and biodegradation [72]. Conversely, the positive impact of the secondary sector involving industrial activities positions coastal MPs as the primary terrestrial source, with various pathways contributing to mangrove pollution [21,73]. Notably, only the primary sector significantly influenced the coloration (black) of MPs at a lower significance level ($p < 0.05$) (Fig. 6b). This indicates that as soil depth increases, the impacts of primary and secondary industrial activities diminish, with only dyes from the primary sector, characterized by relatively slow environmental aging and biodegradation [74], affecting the MPs in the subsoil.

We found that soil temperature, primarily governed by MAT, was positively correlated with MPs (PET) in the topsoil (Fig. 6a), reflecting the temperature-dependent processes involved in MP formation [75]. This correlation diminished in subsoils (Fig. 6a), where MPs—mainly transported vertically from surface sources and subsequently buried by physical [45] or biological [46,47] mechanisms—exhibited largely temperature-independent dynamics. Additionally, clay content was negatively correlated with MPs in both soil layers—a relationship that intensified with depth (Fig. 6a and b). This pattern suggests that clay restricts MP migration in a depth-dependent manner, primarily through physical encapsulation [76]. This mechanism is facilitated by reduced hydrodynamic and biological disturbances in deeper soil layers, promoting the gradual settling and long-term accumulation of fine clay particles. The study revealed that in the topsoil, MPs affected the *mcrA*:*pmoA* ratio through their chemical compositions, whereas in the subsoil, this ratio was influenced by their physical properties (Fig. 6). This shift reflects the distinct growth conditions of CH_4-cycling microorganisms shaped by varying MPs [77], which ultimately impact the balance between methanogens and methanotrophs as well as CH_4 production potential [78]. Additionally, soil temperature and the N:P ratio significantly affected the *mcrA*:*pmoA* ratio (path coefficient $= -0.60$, $p < 0.01$) in the topsoil, whereas clay content became the most influential factor in the subsoil. This shift indicates that the balance between methanogens and methanotrophs is variably influenced by soil physicochemical properties due to stratification [79].

5. Conclusion

In summary, this study elucidates the complex interactions between MPs and CH_4-cycling microbial communities in Chinese mangroves, showing how anthropogenic and environmental factors shape these relationships and influence CH_4 emission potential under global MP pollution conditions. Our findings revealed distinct depth-dependent patterns in MP distribution, with topsoil exhibiting significantly higher MP concentrations and greater diversity in particle characteristics compared to subsoils. Notably, stronger associations were observed in topsoil between MPs and methanogenic microorganisms, supported by more complex microbial co-occurrence networks. Anthropogenic activities, particularly those associated with secondary industries, were found to significantly increase MP accumulation in topsoil, subsequently elevating the *mcrA*:*pmoA* ratio and indicating enhanced CH_4 emission potential. These results underscore the urgent need to implement stringent measures to mitigate land-based plastic discharges from industrial sources. Such measures are essential for optimizing mangrove carbon sequestration capacity and mitigating CH_4 emissions during global restoration projects.

CRediT authorship contribution statement

Xiaotong He: Writing - Original Draft, Resources, Investigation, Formal Analysis, Data Curation. **Shiguang Xu:** Resources, Investigation. **Han Ren:** Writing - Review & Editing. **Xiaobing Yang:** Resources, Investigation. **Feizhou Su:** Validation. **Shuo Gao:** Validation. **Chenxi Xie:** Validation. **Junhui Zhao:** Validation. **Zhan Jin:** Funding acquisition. **Xiangjin Shen:** Writing - Review & Editing. **Rongxiao Che:** Writing - Review & Editing. **Derong Xiao:** Writing - Review & Editing, Writing - Original Draft, Project Administration, Methodology, Funding Acquisition, Data Curation, Conceptualization.

Data availability

The data used for this study are available from the Dryad Digital Repository (http://datadryad.org/share/aYee800YLrgDSEnRvO

R4YsIpZzzWoQJPTqdjEKDW4ao).

Declaration of competing interest

The authors declare that they have no known competing financial interests or personal relationships that could have appeared to influence the work reported in this paper.

Acknowledgements

This work was supported by the “Pioneer” and “Leading Goose” R&D Program of Zhejiang (2024C02002) and the National Natural Science Foundation of China (No. 41867059, 52100197).

Appendix A. Supplementary data

Supplementary data to this article can be found online at https://doi.org/10.1016/j.ese.2025.100593.

References

[1] A.S. Pottinger, R. Geyer, N. Biyani, C.C. Martinez, N. Nathan, M.R. Morse, C. Liu, S. Hu, M. de Bruyn, C. Boettiger, E. Baker, D.J. McCauley, Pathways to reduce global plastic waste mismanagement and greenhouse gas emissions by 2050, Science 386 (6726) (2024) 1168–1173.
[2] B. Gao, H. Yao, Y. Li, Y. Zhu, Microplastic addition alters the microbial community structure and stimulates soil carbon dioxide emissions in vegetable-growing soil, Environ. Toxicol. Chem. 40 (2) (2021) 352–365.
[3] X. Kou, E. Morriën, Y. Tian, X. Zhang, C. Lu, H. Xie, W. Liang, Q. Li, C. Liang, Exogenous carbon turnover within the soil food web strengthens soil carbon sequestration through microbial necromass accumulation, Glob. Change Biol. 29 (14) (2023) 4069–4080.
[4] Y. Li, Y. Tang, W. Qiang, W. Xiao, X. Lian, S. Yuan, Y. Yuan, Q. Wang, Z. Liu, Y. Chen, Effect of tire wear particle accumulation on nitrogen removal and greenhouse gases abatement in bioretention systems: soil characteristics, microbial community, and functional genes, Environ. Res. 251 (2024) 118574.
[5] R. Geyer, J.R. Jambeck, K.L. Law, Production, use, and fate of all plastics ever made, Sci. Adv. 3 (7) (2017) e1700782.
[6] M. Shen, S. Liu, T. Hu, K. Zheng, Y. Wang, H. Long, Recent advances in the research on effects of micro/nanoplastics on carbon conversion and carbon cycle: a review, J. Environ. Manage. 334 (2023) 117529.
[7] T.S. Galloway, M. Cole, C. Lewis, Interactions of microplastic debris throughout the marine ecosystem, Nat. Ecol. Evol. 1 (5) (2017) 116.
[8] J. Lehmann, C.M. Hansel, C. Kaiser, M. Kleber, K. Maher, S. Manzoni, N. Nunan, M. Reichstein, J.P. Schimel, M.S. Torn, W.R. Wieder, I. Kögel-Knabner, Persistence of soil organic carbon caused by functional complexity, Nat. Geosci. 13 (8) (2020) 529–534.
[9] X. Feng, Q. Wang, Y. Sun, S. Zhang, F. Wang, Microplastics change soil properties, heavy metal availability and bacterial community in a Pb-Zn-contaminated soil, J. Hazard. Mater. 424 (2022) 127364.
[10] T. Zhao, Y.M. Lozano, M.C. Rillig, Microplastics increase soil pH and decrease microbial activities as a function of microplastic shape, polymer type, and exposure time, Front. Environ. Sci. 9 (2021) 675803.
[11] M.C. Rillig, E. Leifheit, J. Lehmann, Microplastic effects on carbon cycling processes in soils, PLoS Biol. 19 (3) (2021) e3001130.
[12] M.C. Rillig, A. Lehmann, M. Ryo, J. Bergmann, Shaping up: toward considering the shape and form of pollutants, Environ. Sci. Technol. 53 (14) (2019) 7925–7926.
[13] M.E. Seeley, B. Song, R. Passie, R.C. Hale, Microplastics affect sedimentary microbial communities and nitrogen cycling, Nat. Commun. 11 (1) (2020) 2372.
[14] C. Martin, H. Almahasheer, C.M. Duarte, Mangrove forests as traps for marine litter, Environ. Pollut. 247 (2019) 499.
[15] P.I. Macreadie, M.D.P. Costa, T.B. Atwood, D.A. Friess, J.J. Kelleway, H. Kennedy, C.E. Lovelock, O. Serrano, C.M. Duarte, Blue carbon as a natural climate solution, Nat. Rev. Earth Environ. 2 (12) (2021) 826–839.
[16] G. Qin, Z. Lu, S. Gan, L. Zhang, J. Wu, C.J. Sanders, Z. He, X. Yu, J. Zhang, J. Zhou, R. Ding, X. Huang, H. Chen, H. He, M. Yu, H. Li, F. Wang, Fiddler crab bioturbation stimulates methane emissions in mangroves: insights into microbial mechanisms, Soil Biol. Biochem. 194 (2024) 109445.
[17] X. Yu, X. Yang, Y. Wu, Y. Peng, T. Yang, F. Xiao, Q. Zhong, K. Xu, L. Shu, Q. He, Y. Tian, Q. Yan, C. Wang, B. Wu, Z. He, Sonneratia apetala introduction alters methane cycling microbial communities and increases methane emissions in mangrove ecosystems, Soil Biol. Biochem. 144 (2020) 107775.
[18] L. Zhang, J.M. Adams, M.G. Dumont, Y. Li, Y. Shi, D. He, J.-S. He, H. Chu, Distinct methanotrophic communities exist in habitats with different soil water contents, Soil Biol. Biochem. 132 (2019) 143–152.
[19] J.A. Rosentreter, G.G. Laruelle, H.W. Bange, T.S. Bianchi, J.J.M. Busecke, W.-J. Cai, B.D. Eyre, I. Forbrich, E.Y. Kwon, T. Maavara, N. Moosdorf, R.G. Najjar, V. V.S.S. Sarma, B. Van Dam, P. Regnier, Coastal vegetation and estuaries are collectively a greenhouse gas sink, Nat. Clim. Change 13 (6) (2023) 579–587.
[20] S. Kirschke, P. Bousquet, P. Ciais, M. Saunois, J.G. Canadell, E.J. Dlugokencky, P. Bergamaschi, D. Bergmann, D.R. Blake, L. Bruhwiler, Three decades of global methane sources and sinks, Nat. Geosci. 6 (2013) 813.
[21] Y. Wang, M. Jiao, T. Li, R. Li, B. Liu, Role of mangrove forest in interception of microplastics (MPs): challenges, progress, and prospects, J. Hazard. Mater. 445 (2023) 130636.
[22] C. Martin, F. Baalkhuyur, L. Valluzzi, V. Saderne, M. Cusack, H. Almahasheer, P.K. Krishnakumar, L. Rabaoui, M.A. Qurban, A. Arias-Ortiz, P. Masque, C. M. Duarte, Exponential increase of plastic burial in mangrove sediments as a major plastic sink, Sci. Adv. 6 (44) (2020) eaaz5593.
[23] Y. Wu, X. Chen, L. Wen, Z. Li, M. Peng, H. Wu, L. Xie, Linking human activity to spatial accumulation of microplastics along mangrove coasts, Sci. Total Environ. 825 (2022) 154014.
[24] Y. Zhang, S. Kang, S. Allen, D. Allen, T. Gao, M. Sillanpää, Atmospheric microplastics: a review on current status and perspectives, Earth Sci. Rev. 203 (2020) 103118.
[25] T.B. Atwood, R.M. Connolly, H. Almahasheer, P.E. Carnell, C.M. Duarte, C. J. Ewers Lewis, X. Irigoien, J.J. Kelleway, P.S. Lavery, P.I. Macreadie, O. Serrano, C.J. Sanders, I. Santos, A.D.L. Steven, C.E. Lovelock, Global patterns in mangrove soil carbon stocks and losses, Nat. Clim. Change 7 (7) (2017) 523–528.
[26] Z. Deng, P. Ciais, Z.A. Tzompa-Sosa, M. Saunois, C. Qiu, C. Tan, T. Sun, P. Ke, Y. Cui, K. Tanaka, X. Lin, R.L. Thompson, H. Tian, Y. Yao, Y. Huang, R. Lauerwald, A.K. Jain, X. Xu, A. Bastos, S. Sitch, P.I. Palmer, T. Lauvaux, A. d'Aspremont, C. Giron, A. Benoit, B. Poulter, J. Chang, A.M.R. Petrescu, S. J. Davis, Z. Liu, G. Grassi, C. Albergel, F.N. Tubiello, L. Perugini, W. Peters, F. Chevallier, Comparing national greenhouse gas budgets reported in UNFCCC inventories against atmospheric inversions, Earth Syst. Sci. Data 14 (4) (2022) 1639–1675.
[27] S.D. Sasmito, M. Basyuni, A. Kridalaksana, M.F. Saragi-Sasmito, C.E. Lovelock, D. Murdiyarso, Challenges and opportunities for achieving sustainable development goals through restoration of Indonesia's mangroves, Nat. Ecol. Evol. 7 (1) (2023) 62–70.
[28] M. Gong, N. Teller, E.J. Golebie, M. Aczel, Z. Jiang, J. Van Zeghbroeck, J. Liu, Unveiling complementarities between mangrove restoration and global sustainable development goals, J. Cleaner Prod. 474 (2024) 143524.
[29] The State Council, The state concil, the People'S Republic of China. China to Build, Restore 18,800 Hectares of Mangrove by 2025, 2020.
[30] M. Jia, Z. Wang, D. Mao, C. Huang, C. Lu, Spatial-temporal changes of China's mangrove forests over the past 50 years: an analysis towards the sustainable development goals (SDGs), Chin. Sci. Bull. 66 (30) (2021) 3886–3901.
[31] C. Li, F. Wang, P. Yang, F. Wang, Y. Hu, Y. Zhao, L. Tian, R. Zhao, Mangrove wetlands distribution status identification, changing trend analyzation and carbon storage assessment of China, China Geol. 7 (1) (2024) 1–11.
[32] National Bureau of Statistics of China, China city statistical yearbook: 2018, in: Department of Urban socio-economic Survey of the National Bureau of Statistics, China Statistics Press, Beijing, 2019, pp. 357–364.
[33] National Bureau of Statistics of China, China city statistical yearbook: 2019, in: Department of Urban socio-economic Survey of the National Bureau of Statistics, China Statistics Press, Beijing, 2020, pp. 359–366.
[34] National Bureau of Statistics of China, China city statistical yearbook: 2020, in: Department of Urban socio-economic Survey of the National Bureau of Statistics, China Statistics Press, Beijing, 2021, pp. 271–279.
[35] National Bureau of Statistics of China, China city statistical yearbook: 2021, in: Department of Urban socio-economic Survey of the National Bureau of Statistics, China Statistics Press, Beijing, 2022, pp. 287–295.
[36] National Bureau of Statistics of China, China city statistical yearbook: 2022, in: Department of Urban socio-economic Survey of the National Bureau of Statistics, China Statistics Press, Beijing, 2023, pp. 287–295.
[37] S.E. Fick, R.J. Hijmans, WorldClim 2: new 1-km spatial resolution climate surfaces for global land areas, Int. J. Climatol. 37 (12) (2017) 4302–4315.
[38] S. Bao, Agro-Chemical Analysis of Soil, China Agricultural Press, Beijing, 2000.
[39] X. Wu, J. Yang, H. Ruan, S. Wang, Y. Yang, I. Naeem, L. Wang, L. Liu, D. Wang, The diversity and co-occurrence network of soil bacterial and fungal communities and their implications for a new indicator of grassland degradation, Ecol. Indic. 129 (2021) 107989.
[40] Y. Benjamini, A.M. Krieger, D. Yekutieli, Adaptive linear step-up procedures that control the false discovery rate, Biometrika 93 (3) (2006) 491–507.
[41] Z. Han, P. Xu, Z. Li, H. Lin, C. Zhu, J. Wang, J. Zou, Microbial diversity and the abundance of keystone species drive the response of soil multifunctionality to organic substitution and biochar amendment in a tea plantation, Glob. Change Biol. Bioenergy 14 (4) (2022) 481–495.
[42] Y. Lin, L. Wang, B. Lin, B. Liu, T. Guan, S. Guo, Q. Li, C. Wei, Differences in the uptake and translocation of differentially charged microplastics by the taproot and lateral root of mangroves, Sci. Total Environ. 945 (2024) 174113.
[43] M. Rujnić-Sokele, A. Pilipović, Challenges and opportunities of biodegradable plastics: a mini review, Waste Manage. Res. 35 (2) (2017) 132–140.
[44] I. Azeem, M. Adeel, M.A. Ahmad, N. Shakoor, G.D. Jiangcuo, K. Azeem, M. Ishfaq, A. Shakoor, M. Ayaz, M. Xu, Y. Rui, Uptake and accumulation of nano/microplastics in plants: a critical review, Nanomaterials 11 (11) (2021).
[45] M.A.K. Jansen, A.L. Andrady, J.F. Bornman, P.J. Aucamp, A.F. Bais, A.

T. Banaszak, P.W. Barnes, G.H. Bernhard, L.S. Bruckman, R. Busquets, D.-P. Häder, M.L. Hanson, A.M. Heikkilä, S. Hylander, R.M. Lucas, R. Mackenzie, S. Madronich, P.J. Neale, R.E. Neale, C.M. Olsen, R. Ossola, K.K. Pandey, I. Petropavlovskikh, L.E. Revell, S.A. Robinson, T.M. Robson, K.C. Rose, K. R. Solomon, M.P.S. Andersen, B. Sulzberger, T.J. Wallington, Q.-W. Wang, S.-Å. Wängberg, C.C. White, A.R. Young, R.G. Zepp, L. Zhu, Plastics in the environment in the context of UV radiation, climate change and the montreal protocol: UNEP environmental effects assessment panel, update 2023, Photochem. Photobiol. Sci. 23 (4) (2024) 629–650.

[46] K. Kvale, A.E.F. Prowe, C.T. Chien, A. Landolfi, A. Oschlies, Zooplankton grazing of microplastic can accelerate global loss of ocean oxygen, Nat. Commun. 12 (1) (2021) 2358.

[47] A. Delacuvellerie, V. Cyriaque, S. Gobert, S. Benali, R. Wattiez, The plastisphere in marine ecosystem hosts potential specific microbial degraders including Alcanivorax borkumensis as a key player for the low-density polyethylene degradation, J. Hazard. Mater. 380 (2019) 120899.

[48] J. Li, W. Huang, Y. Xu, A. Jin, D. Zhang, C. Zhang, Microplastics in sediment cores as indicators of temporal trends in microplastic pollution in andong salt marsh, Hangzhou Bay, China, Reg. Stud. Mar. Sci. 35 (2020) 101149.

[49] J. Lloret, R. Pedrosa-Pamies, N. Vandal, R. Rorty, M. Ritchie, C. McGuire, K. Chenoweth, I. Valiela, Salt marsh sediments act as sinks for microplastics and reveal effects of current and historical land use changes, Environ. Adv. 4 (2021) 100060.

[50] L. Viet Dung, T. Huu Duc, L. Thi Khanh Linh, T. Thi Dieu Ly, H. Anh Duong, N. Thi My Hao, Depth profiles of microplastics in sediment cores from two mangrove forests in Northern Vietnam, J. Mar. Sci. Eng. 9 (2021).

[51] L. Qian, X. Yu, H. Gu, F. Liu, Y. Fan, C. Wang, Q. He, Y. Tian, Y. Peng, L. Shu, S. Wang, Z. Huang, Q. Yan, J. He, G. Liu, Q. Tu, Z. He, Vertically stratified methane, nitrogen and sulphur cycling and coupling mechanisms in mangrove sediment microbiomes, Microbiome 11 (1) (2023) 71.

[52] R. Chauhan, A. Datta, A.L. Ramanathan, T.K. Adhya, Whether conversion of mangrove forest to rice cropland is environmentally and economically viable? Agric. Ecosyst. Environ. 246 (2017) 38–47.

[53] S.D. Sasmito, P. Taillardat, J.N. Clendenning, C. Cameron, D.A. Friess, D. Murdiyarso, L.B. Hutley, Effect of land-use and land-cover change on mangrove blue carbon: a systematic review, Glob. Change Biol. 25 (12) (2019) 4291–4302.

[54] Y. Yang, W. Wang, Q. Hu, X. Yao, W. Yang, S. Wen, H. Wu, J. Jin, L. Shen, Conversion of coastal wetlands to paddy fields substantially decreases methane oxidation potential and methanotrophic abundance on the eastern coast of China, Water Res. 272 (2025) 122962.

[55] R. Wagner, D. Zona, W. Oechel, D. Lipson, Microbial community structure and soil pH correspond to methane production in arctic Alaska soils, Environ. Microbiol. 19 (8) (2017) 3398–3410.

[56] L. Zeng, J. Tian, H. Chen, N. Wu, Z. Yan, L. Du, Y. Shen, X. Wang, Changes in methane oxidation ability and methanotrophic community composition across different climatic zones, J. Soils Sediments 19 (2) (2019) 533–543.

[57] R. Laiho, P. Salovaara, P. Mäkiranta, K. Peltoniemi, T. Penttilä, T. Rajala, J. Hultman, M. Korkiakoski, H. Fritze, Reindeer shape soil methanogenic and methanotrophic communities in subarctic fen peatlands, with a minor impact on methane emissions — a field study, Soil Biol. Biochem. 199 (2024) 109590.

[58] K. Peltoniemi, R. Laiho, H. Juottonen, L. Bodrossy, D.K. Kell, K. Minkkinen, P. Mäkiranta, L. Mehtätalo, T. Penttilä, H.M.P. Siljanen, E.-S. Tuittila, T. Tuomivirta, H. Fritze, Responses of methanogenic and methanotrophic communities to warming in varying moisture regimes of two boreal fens, Soil Biol. Biochem. 97 (2016) 144–156.

[59] F.T. de Vries, R.I. Griffiths, M. Bailey, H. Craig, M. Girlanda, H.S. Gweon, S. Hallin, A. Kaisermann, A.M. Keith, M. Kretzschmar, P. Lemanceau, E. Lumini, K.E. Mason, A. Oliver, N. Ostle, J.I. Prosser, C. Thion, B. Thomson, R. D. Bardgett, Soil bacterial networks are less stable under drought than fungal networks, Nat. Commun. 9 (1) (2018) 3033.

[60] B.W.G. Stone, P. Dijkstra, B.K. Finley, R. Fitzpatrick, M.M. Foley, M. Hayer, K. S. Hofmockel, B.J. Koch, J. Li, X.J.A. Liu, A. Martinez, R.L. Mau, J. Marks, V. Monsaint-Queeney, E.M. Morrissey, J. Propster, J. Pett-Ridge, A.M. Purcell, E. Schwartz, B.A. Hungate, Life history strategies among soil bacteria—dichotomy for few, continuum for many, ISME J. 17 (4) (2023) 611–619.

[61] T. Qin, Y. Liu, R. Hu, K. Yang, B. Zheng, J. Li, Z. Liu, P. Li, T. Ma, K. Xiong, J. Liang, Z. Rang, J. Li, Reduction of soil methane emissions from croplands with 20–40 years of cultivation mediated by methane-metabolizing microorganisms, J. Cleaner Prod. 435 (2024) 140489.

[62] H. Wang, Y. Zhong, Q. Yang, J. Li, D. Li, J. Wu, S. Yang, J. Liu, Y. Deng, J. Song, P. a. Peng, Coupling of sulfate reduction and dissolved organic carbon degradation accelerated by microplastics in blue carbon ecosystems, Water Res. 279 (2025) 123414.

[63] X. Zhou, C. Xiao, B. Zhang, X. Yang, Depth-dependent response of soil microbial community and greenhouse gas efflux to polylactic acid microplastics and tidal cycles in a mangrove ecosystem, J. Hazard. Mater. 489 (2025) 137664.

[64] H. Xie, J. Chen, L. Feng, L. He, C. Zhou, P. Hong, S. Sun, H. Zhao, Y. Liang, L. Ren, Y. Zhang, C. Li, Chemotaxis-selective colonization of mangrove rhizosphere microbes on nine different microplastics, Sci. Total Environ. 752 (2021) 142223.

[65] C. Fang, Y. He, Y. Yang, B. Fu, S. Pan, F. Jiao, J. Wang, H. Yang, Laboratory tidal microcosm deciphers responses of sediment archaeal and bacterial communities to microplastic exposure, J. Hazard. Mater. 458 (2023) 131813.

[66] C. Fang, Y. Yang, S. Zhang, Y. He, S. Pan, L. Zhou, J. Wang, H. Yang, Unveiling the impact of microplastics with distinct polymer types and concentrations on tidal sediment microbiome and nitrogen cycling, J. Hazard. Mater. 472 (2024) 134387.

[67] M.-M. Chen, F.-H. Nie, A. Qamar, D.-h. Zhu, Y. Hu, M. Zhang, Q.-L. Song, H.-Y. Lin, Z.-B. Chen, S.-Q. Liu, J.-J. Chen, Effects of microplastics on microbial community in zhanjiang mangrove sediments, Bull. Environ. Contam. Toxicol. 108 (5) (2022) 867–877.

[68] X. Zhou, C. Xiao, B. Zhang, T. Chen, X. Yang, Effects of microplastics on carbon release and microbial community in mangrove soil systems, J. Hazard. Mater. 465 (2024) 133152.

[69] X. Lin, S. Lin, L. Peng, M. Chen, X. Cheng, S. Xie, R. Bao, Y. Su, T. Mehmood, Effects of polypropylene microplastics on carbon dioxide dynamics in intertidal mangrove sediments, Environ. Pollut. 346 (2024) 123682.

[70] Z. Ouyang, S. Li, J. Xue, J. Liao, C. Xiao, H. Zhang, X. Li, P. Liu, S. Hu, X. Guo, L. Zhu, Dissolved organic matter derived from biodegradable microplastic promotes photo-aging of coexisting microplastics and alters microbial metabolism, J. Hazard. Mater. 445 (2023) 130564.

[71] S. Wang, X. Wang, M. Fessler, B. Jin, Y. Su, Y. Zhang, Insights into the impact of polyethylene microplastics on methane recovery from wastewater via bioelectrochemical anaerobic digestion, Water Res. 221 (2022) 118844.

[72] J. Lofty, V. Muhawenimana, C.A.M.E. Wilson, P. Ouro, Microplastics removal from a primary settler tank in a wastewater treatment plant and estimations of contamination onto European agricultural land via sewage sludge recycling, Environ. Pollut. 304 (2022) 119198.

[73] R. Li, L. Zhang, B. Xue, Y. Wang, Abundance and characteristics of microplastics in the mangrove sediment of the semi-enclosed maowei sea of the South China sea: new implications for location, rhizosphere, and sediment compositions, Environ. Pollut. 244 (2019) 685–692.

[74] B. Klun, U. Rozman, G. Kalčíková, Environmental aging and biodegradation of tire wear microplastics in the aquatic environment, J. Environ. Chem. Eng. 11 (5) (2023) 110604.

[75] M. Sivaraman, L. Fan, W. Yan, Quantitative analysis of microplastics in beach sand via low-temperature solvent extraction and thermal degradation: effects of particle size and sample depth, Sci. Total Environ. 953 (2024) 176009.

[76] S. Ren, W. Kai, Z. Jinrui, L. Jingjing, Z. Hanyue, Q. Ruimin, X. Wen, Y. Changrong, L. Xuejun, Z. Fusuo, J.D.L., D.R., Chadwick, Potential sources and occurrence of macro-plastics and microplastics pollution in farmland soils: a typical case of China, Crit. Rev. Environ. Sci. Technol. 54 (7) (2024) 533–556.

[77] D.R. Finn, M. Ziv-El, J. van Haren, J.G. Park, J. del Aguila-Pasquel, J. D. Urquiza–Muñoz, H. Cadillo-Quiroz, Methanogens and methanotrophs show nutrient-dependent community assemblage patterns across tropical peatlands of the pastaza-marañón basin, Peruvian Amazonia, Front. Microbiol. 11 (2020) 746.

[78] H. Luo, Y. Li, Y. Zhao, Y. Xiang, D. He, X. Pan, Effects of accelerated aging on characteristics, leaching, and toxicity of commercial lead chromate pigmented microplastics, Environ. Pollut. 257 (2020) 113475.

[79] X. Yao, W. Wang, Y. Yang, W. Yang, Q. Hu, J. Jin, J. Liu, Y. Wang, L. Shen, Stimulation of methane production potential and alteration in community composition of methanogens following conversion of China's coastal marshes to paddy fields, Catena 246 (2024) 108428.

[80] J. Li, H. Zhang, K. Zhang, R. Yang, R. Li, Y. Li, Characterization, source, and retention of microplastic in sandy beaches and mangrove wetlands of the Qinzhou Bay, China, Mar. Pollut. Bull. 136 (2018) 401.

[81] P. Dou, L. Mai, L. Bao, E.Y. Zeng, Microplastics on beaches and mangrove sediments along the coast of South China, Mar. Pollut. Bull. 172 (2021) 112806.

[82] X. Liu, H. Liu, L. Chen, X. Wang, Ecological interception effect of mangroves on microplastics, J. Hazard. Mater. 423 (2022) 127231.

[83] Y. Li, R. Huang, L. Hu, C. Zhang, X. Xu, L. Song, Z. Wang, X. Pan, G. Christakos, J. Wu, Microplastics distribution in different habitats of Ximen Island and the trapping effect of blue carbon habitats on microplastics, Mar. Pollut. Bull. 181 (2022) 113912.

[84] X. Zhang, X. Xia, M. Dai, J. Cen, L. Zhou, J. Xie, Microplastic pollution and its relationship with the bacterial community in coastal sediments near Guangdong province, South China, Sci. Total Environ. 760 (2021) 144091.

[85] Y. Huang, X. Xiao, C. Xu, Y.D. Perianen, J. Hu, M. Holmer, Seagrass beds acting as a trap of microplastics - emerging hotspot in the coastal region? Environ. Pollut. 257 (2020) 113450.

[86] Y. Huang, X. Xiao, K. Effiong, C. Xu, Z. Su, J. Hu, S. Jiao, M. Holmer, New insights into the microplastic enrichment in the blue carbon ecosystem: evidence from seagrass meadows and mangrove forests in coastal South China Sea, Environ. Sci. Technol. 55 (8) (2021) 4804.

[87] M.A. Fraser, L. Chen, M. Ashar, W. Huang, J. Zeng, C. Zhang, D. Zhang, Occurrence and distribution of microplastics and polychlorinated biphenyls in sediments from the Qiantang river and Hangzhou Bay, China, Ecotoxicol. Environ. Saf. 196 (2020) 110536.